Digermane Deposition on Si(100) and Ge(100): from Adsorption Mechanism to Epitaxial Growth

ARTICLE *in* THE JOURNAL OF PHYSICAL CHEMISTRY C · DECEMBER 2013

Impact Factor: 4.77 · DOI: 10.1021/jp410145u

12 AUTHORS, INCLUDING:

Roberto C. Longo
University of Texas at Dallas
27 PUBLICATIONS **144** CITATIONS
SEE PROFILE

Stephen J Mcdonnell
University of Texas at Dallas
65 PUBLICATIONS **1,362** CITATIONS
SEE PROFILE

Xiaoye Qin
University of Texas at Dallas
24 PUBLICATIONS **163** CITATIONS
SEE PROFILE

Kyeongjae Cho
University of Texas at Dallas
302 PUBLICATIONS **9,400** CITATIONS
SEE PROFILE

THE JOURNAL OF PHYSICAL CHEMISTRY C

Article

pubs.acs.org/JPCC

Digermane Deposition on Si(100) and Ge(100): from Adsorption Mechanism to Epitaxial Growth

Don Dick,[†] Jean-Francois Veyan,[‡] R. C. Longo,[‡] Stephen McDonnell,[‡] Josh B. Ballard,[§] Xiaoye Qin,[‡] Hong Dong,[‡] James H. G. Owen,[§] John N. Randall,[§] Robert M. Wallace,[‡] Kyeongjae Cho,[‡] and Yves J. Chabal*[,‡]

[†]Physics Department, University of Texas at Dallas, 800 W Campbell Road, Richardson, Texas 75080, United States

[‡]Materials Science and Engineering Department, University of Texas at Dallas, 800 West Campbell Road, Richardson, Texas 75080, United States

[§]Zyvex Laboratories, LLC, 1321 North Plano Road, Richardson, Texas 75081, United States

Supporting Information

ABSTRACT: Controlled fabrication of nanometer-scale devices such as quantum dots and nanowires requires an understanding of the initial chemisorption mechanisms involved in epitaxial growth. Vapor phase epitaxy can provide controlled deposition when using precursors that are not reactive with the H-terminated surfaces at ambient temperatures. For instance, digermane (Ge_2H_6) has potential as such a precursor for Ge ALE on Si(100) surfaces at moderate temperatures; yet, its adsorption configuration and subsequent decomposition pathways are not well understood. In situ Fourier transform infrared spectroscopy and first principles calculations reveal that Ge_2H_6 chemisorbs through a β-hydride elimination mechanism, forming Ge_2H_5 and H on both Si(100)-(2 × 1) and Ge(100)-(2 × 1) surfaces, instead of the previously proposed Ge−Ge bond breaking mechanism, and subsequently decomposes into an ad-dimer. The resulting coverage of Ge after a saturation exposure is estimated to be about 0.3 monolayers. Interestingly, the decomposition of adsorbed Ge_2H_5 on Si(100) is faster than Si_2H_5 on Ge(100) at 173 K. The desorption temperature of hydrogen on Si(100) is shown to depend on the Ge coverage, falling from 698 K for ∼1/4 ML Ge on Si(100) to 573 K for a nearly full Ge coverage, consistent with H desorption on Ge(100). Furthermore, hydrogen is observed to migrate from Ge to Si, prior to desorption. This property opens the door for selective growth of Ge on patterned H-terminated Si surfaces.

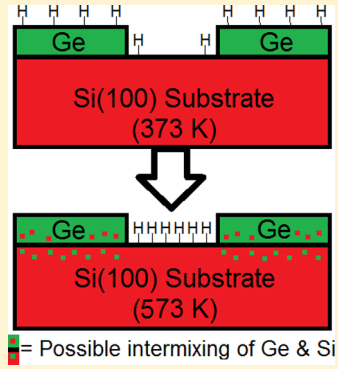

INTRODUCTION

Selective depassivation of hydrogen on H-terminated Si(100) surfaces with nanoscale precision, e.g., with a scanning tunneling microscopy (STM) tip, is a powerful technique to nanopattern Si(111)[1] and Si(100)[2] surfaces. Once the Si surface is depassivated, material can be deposited on the clean areas by selective vapor phase processing because H-terminated Si surfaces remain stable (unreactive) at moderate temperatures (<550 K). Among several methods for growing materials in such regions including atomic layer[3−5] and chemical vapor[6−8] deposition (ALD and CVD), atomic layer epitaxy (ALE)[9] is attractive using gases such as disilane and digermane when STM is used to remove intermediate surface hydrogen atoms, as recently shown for disilane.[10]

Heteroepitaxy of Ge films on Si has been extensively studied,[11] starting in the 80s as it constituted the basis of optoelectronic devices. Various techniques have been used to investigate Ge/Si(100) such as X-ray photoelectron spectroscopy[12,13] (XPS), ultraviolet photoelectron spectroscopy[14] (UPS), scanning tunneling microscopy[15,16] (STM), high resolution core-level photoemission spectroscopy,[15,16] and temperature programmed desorption[13,17] (TPD). Despite the usefulness of Fourier transform infrared (FT-IR) spectroscopy to provide direct information on hydride species of adsorbed digermane, only one such study was performed by Lu et al.[18] for digermane chemisorption. In this and all other studies of digermane adsorption, it was assumed that the initial chemisorption step in the decomposition of gaseous digermane on Si(100) and Ge(100) surfaces involved the breaking of the Ge−Ge bond to form two GeH_3* radicals stabilized on the surface dimers. Similarly, experimental studies had also suggested that disilane initially chemisorbs on Si(100) and Ge(100) through Si−Si bond scission,[19−25] although these findings have subsequently been refuted by Veyan et al.[10]

Density functional theory (DFT) studies using nudged elastic band (NEB) calculations[26−28] have shown that the kinetic barrier for chemisorption of disilane on Si(100) though the Si−Si intrabond scission ($Si_2H_6 \rightarrow 2SiH_3$*) was nearly twice as large as it would have been for initial chemisorption through the β-hydride elimination pathway (β-HEP, $Si_2H_6 \rightarrow$

Received: October 12, 2013
Revised: December 10, 2013
Published: December 11, 2013

Si_2H_5* + H*) on Si(100). Therefore, theory supports the interpretation of the recent IR measurements of disilane on Si(100) and Ge(100) surfaces[10] and suggests that the same should occur for digermane on both substrates. However, even though Si and Ge do share very similar outer electron structure, their surface chemistry can be quite different, as illustrated, for instance, with water adsorption on Si(100) and Ge(100).[29,30] It is therefore important to examine systematically the adsorption process of digermane throughout the adsorption and subsequent decomposition processes to determine its use for selective ALE.

We have combined FT-IR spectroscopy and DFT to investigate the initial chemisorption pathway of digermane on Si(100) and Ge(100) surfaces and the subsequent thermal evolution of the adsorbed species, up to complete hydrogen desorption. Our results show that the initial chemisorption of digermane is through the same β-HEP ($Ge_2H_6 \rightarrow Ge_2H_5$* + H*) as has recently been observed for disilane on these surfaces. The evolution of the adsorbed species is then explored by monitoring the hydrogen vibrations from the initial deposition of digermane to full hydrogen desorption via thermal annealing. Conditions for complete Ge coverage of clean Si(100) surfaces using digermane are established by intermediate annealing steps to remove hydrogen from Ge. We find that ~1/3 monolayer Ge (i.e., saturation exposure) is deposited on clean surfaces per cycle. Furthermore, hydrogen is observed to migrate from adsorbed Ge to the available Si sites of the remaining surface before finally desorbing. The annealing temperature required to remove all adsorbed hydrogen is lowered from 698 K (first cycle) to 573 K (10th cycle) as the Ge coverage increases with the number of digermane cycles. The properties of the Ge layer obtained by multiple cycles of digermane exposure and annealing is compared to a bulk Ge(100) surface. Finally, the role of Ge as a surfactant on Si is explored by examining the diffusion of Si on Ge surfaces, including Si surfaces covered by ultrathin Ge layers.

EXPERIMENTAL AND THEORETICAL METHODS

Infrared Absorption Measurements. The 3.8 cm × 1.5 cm ×500 μm double side polished Ge(100) and Si(100) samples are cleaned and reoxidized in the same manner as described in a prior study.[10] The oxidized Si(100) and Ge(100) samples are inserted into the UHV chamber described below and either annealed to 873 K for 6 h (Si samples) or 573 K for 12 h (Ge samples) in order to thoroughly degas the sample holder. Finally, the sample is flashed to either ~1300 (for Si samples) or ~950 K (for Ge samples) in order to remove the protective oxide layer.

The in situ FT-IR measurements are performed in the same ultrahigh vacuum (UHV) chamber as described in a prior study[10] at a base pressure of 2×10^{-10} Torr. A mercury cadmium telluride (MCT-B) detector is used unless otherwise stated. This detector allows for a maximum sensitivity and an absorbance noise level of 1×10^{-5} around 2000 cm^{-1} with a cut off at low wavenumbers of 500 cm^{-1}. By averaging over 1000 scans per spectrum at a resolution of 4 cm^{-1}, a noise level in the Si−H stretch spectrum of about ±4% of a saturation coverage is obtained (see the Supporting Information for an explanation of errors).

The digermane flux on the samples is controlled by a capillary doser (Figure 1). A precision leak valve allows for a controlled pressure, as monitored by a Baratron gauge, to be established in the small leak valve volume (LVV ≈ 560 cm^3).

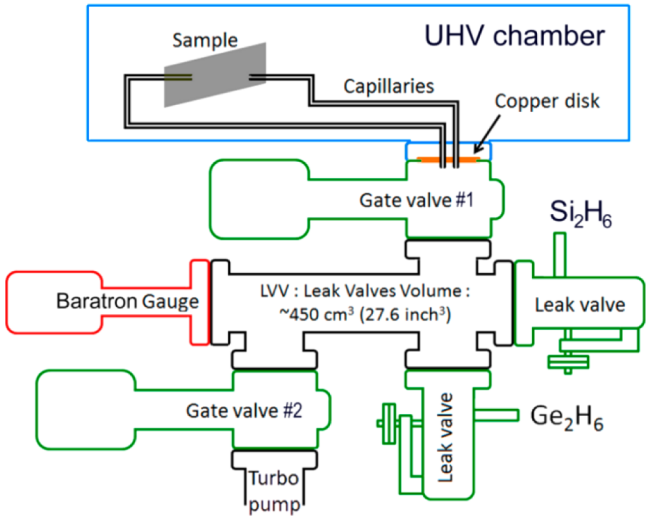

Figure 1. Schematic of the experimental system. Two UHV leak valves (One for Si_2H_6, one for Ge_2H_6) are connected to a buffering volume (LVV). The LVV can be totally closed by gate valves, so the pressure inside its volume is stabilized at the desired value. Then the valve toward the UHV chamber is open and the gas escapes the LVV through capillaries facing each side of the sample inside the UHV chamber.

After reaching a set pressure in the LVV, opening gate valve #1 allows for the digermane gas to flow onto the sample via capillaries that face both sides of the sample. The pressure at the sample surface is estimated to be ~3 orders of magnitude lower than the pressure in the LVV (e.g., ~10^{-5} Torr if the LVV pressure is 10^{-2} Torr). All digermane exposures are performed with 10 mTorr digermane in the LVV (10^{-5} Torr at sample surface) for 30 s, corresponding to 300 Langmuirs per exposure.

In addition to the adsorption and thermal annealing procedures (single exposures) described in the initial chemisorption and thermal decomposition sections, multiple exposures are also performed with aim to build up the Ge coverage on Si(100) through an Ge ALE process with the following sequence:

1. Full digermane saturation of the substrate at a selected temperature (173 or 373 K), i.e., with the equivalent of 10^{-5} Torr at the substrate surface.
2. Data acquisition at the exposure temperature.
3. Sample annealing to 523 K (unless otherwise stated) and with subsequent steps of 50 K until all hydrogen is removed from the surface.
4. Data acquisition after each annealing step at 373 K (requiring cooling after each step).
5. After removal of all hydrides (note that the required temperature varies on Ge coverage), sample cooling to the selected temperature (173 or 373 K).
6. Deposition sequence repeated until no more Si−H is detectable.

Theoretical Methods. In order to calculate the energy barriers and transition states of digermane deposition on Si(100), DFT calculations are performed by applying the nudged elastic band (NEB) method,[31] as part of the VASP (Vienna ab-initio simulation package) code.[32−34] We use the same functional, pseudopotential, k-point mesh, and supercell slab geometries as was done for the calculations of disilane

dx.doi.org/10.1021/jp410145u | J. Phys. Chem. C 2014, 118, 482−493

adsorption on Si(100) and Ge(100) studied previously,[10] to be able to obtain a quantitative comparison.

Briefly, the generalized gradient approximation (GGA)-corrected PW91 approximation[35] for the exchange and correlation functional was used to model the electron-ion interactions described by ultrasoft pseudopotentials[36] with a cutoff energy of 400 eV. A k-point mesh with (12 × 12 × 1) grids generated by the Monkhorst-Pack scheme[37] was used in these calculations. The geometry of the Si(100) supercell slab consisted of 6 layers of Si atoms with the bottom surface passivated by two hydrogen atoms on each Si site and a vacuum thickness of 12 Å separating each side of the slab. All Ge hydrides (e.g., Ge_2H_5, H, GeH_3, and GeH_2) were adsorbed only on the upper side of the slab. The supercell was allowed to relax keeping the bottom H and Si layers fixed to the experimental lattice constant (5.431 Å).

RESULTS AND INTERPRETATION

The description of the vibrational modes of the possible structures formed in the adsorption and decomposition processes of digermane on Si(100) and Ge(100) surfaces can quickly become overly complicated. In order to mitigate this, we adopt the nomenclature initially proposed by Veyan et al.[10] to describe the possible surface configurations of the decomposed disilane species. Briefly, upper case letters (A, B, C, D, and E) are used to assign the possible surface configurations for the digermane species (see Figure 2). For

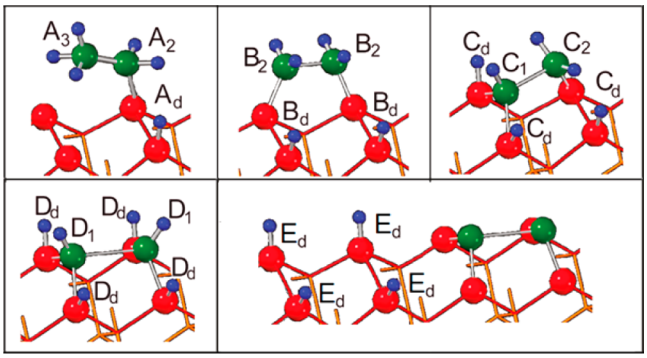

Figure 2. Representation of adsorbed digermane species and their subsequent decomposition. The letters A–E represent the different hydride species described in this section. Green represents Ge atoms, while the red atoms represent the surface (Si or Ge) atoms.

instance, configuration A is assigned to the initial chemisorption of digermane through the β-HEP ($Ge_2H_6 \rightarrow Ge_2H_5$* + H*). The infrared modes that may be detected are assigned by making use of the configuration letter with a subscript identifying how many hydrogen atoms take part in the vibrational mode and a superscript of either δn or νn where δ is for the bending modes, ν is for stretching modes, and n is the nth mode of that vibration. For example, $A_3^{\nu 1}$ describes the first mode of the GeH_3 stretching vibration in the Ge_2H_5* species adsorbed to either Si(100) or Ge(100) surface. In order to distinguish the monohydride species of configurations C, D, and E, a subscript d is used throughout when the hydrogen is bonded to a surface atom in the initial substrate (e.g., $A_d^{\nu 1}$ and $C_d^{\nu 1}$) and a subscript of 1 is used when the hydrogen atom is bonded to the adsorbed Ge (e.g., $C_1^{\nu 1}$).

1. Initial Adsorption at 173 K. A saturation exposure of digermane to Si(100) and Ge(100) surfaces is performed with an effective pressure at the sample surface of 10^{-5} Torr with the sample temperature at 173 K. This allowed for the saturation coverage to be reached in under 2 s, i.e., after 15 L. Figure 3a shows the resulting FT-IR absorbance spectra for this saturation digermane exposure to Si(100) (top gray curve labeled "Si") and Ge(100) (bottom red curve labeled "Ge"). Two spectral regions are shown in this figure: the left panel shows the region containing the Si–H_x and Ge–H_x stretching modes (ν: 2200–1920 cm^{-1}), and the right panel shows the region containing the Si–H_x and Ge–H_x bending modes (δ: 1000–500 cm^{-1}). Distinct modes near 2093 and 630 cm^{-1} can be detected upon Ge_2H_6 exposure to the Si surface; the corresponding modes on the Ge surface are red-shifted by 120 and 70 cm^{-1}, respectively. Previous studies[30] with monohydride termination on Si(100) and Ge(100) allow for ready assignment of these modes to Si–H (2093 cm^{-1} stretching, 635 cm^{-1} bending) and Ge–H (1975 cm^{-1} stretching and 560 cm^{-1} bending) for the Si and Ge surfaces, respectively. The spectra in Figure 3a are further characterized by similar modes near 2067, 2040, 865, 840, 780, and 615 cm^{-1} on both the Si and Ge surfaces.

Figure 3b shows that the adsorption of digermane on Si(100) and Ge(100) at 173 K (Figure. 3a has similar bands to that of disilane on Si(100) and Ge(100) at the same temperature. Figure 3b, previously presented by Veyan et al.,[10] is reproduced here for convenience and highlights two spectral regions: the left panel is for the Si–H stretching mode region (ν: 2200–1920 cm^{-1}), and the right panel for the bending modes region (δ: 1000–500 cm^{-1}); as in Figure 3a. Briefly, the two spectra for Si and Ge substrates are characterized by very similar modes at 2150, 928, 908, 860, and around 700–690 cm^{-1}. For disilane adsorption, DFT calculations clearly showed that all the spectral features common to both substrates were well accounted for by the normal modes of Si_d-Si_2H_5. Importantly, the red shift of the modes observed at 2096 cm^{-1} and 630 cm^{-1} upon Si_2H_6 exposure of a Si surface on a Ge substrate (as highlighted by the black arrow in Figure 3b unambiguously showed that one hydrogen from disilane was transferred to a substrate atom. As calculated in that study by DFT methods and in accordance with previous findings,[10] these spectral features were attributed to Si_d-H monohydride on Si (stretch: A_d^{ν} (Si_d–H) at 2096 cm^{-1}; bend: A_d^{δ} (Si_d–H) at 630–640 cm^{-1}) and Ge_d-H monohydride on Ge (stretch: A_d^{ν} (Ge_d–H) at 1975 cm^{-1}; bend: A_d^{δ} (Ge_d–H) at 550 cm^{-1}), for the Si and Ge substrates, respectively. These data provided unambiguous evidence for the existence of both Si_2H_5 and Si_d-H or Ge_d-H.

The data in Figure 3b for disilane[10] can be directly compared with those presented on Figure 3a for digermane. As expected, the features of digermane adsorption are red-shifted from their disilane counterparts by 85 cm^{-1} in the stretching region and 70 cm^{-1} in the bending region. By making use of this shift in modes, we can assign the modes at 2067, 865, 840, and 780 cm^{-1} to the GeH_3 species in the Ge_2H_5 configuration (A_3), and the mode near 615 cm^{-1} to the GeH_2 species in the Ge_2H_5 configuration (A_2). Furthermore, the modes near 2040 and 2020 cm^{-1} can be ascribed to the GeH_2 species in that same Ge_2H_4 configuration (B_2). Some very specific modes remain at the same frequencies as the disilane counterparts: 2096 and 630 cm^{-1} for the Si substrate and 1975 and 560 cm^{-1} for the Ge substrate. These modes are assigned to monohydride species formed on the substrate surface atoms respectively Si_d-H on Si(100) and Ge_d-H on Ge(100).

dx.doi.org/10.1021/jp410145u | J. Phys. Chem. C 2014, 118, 482–493

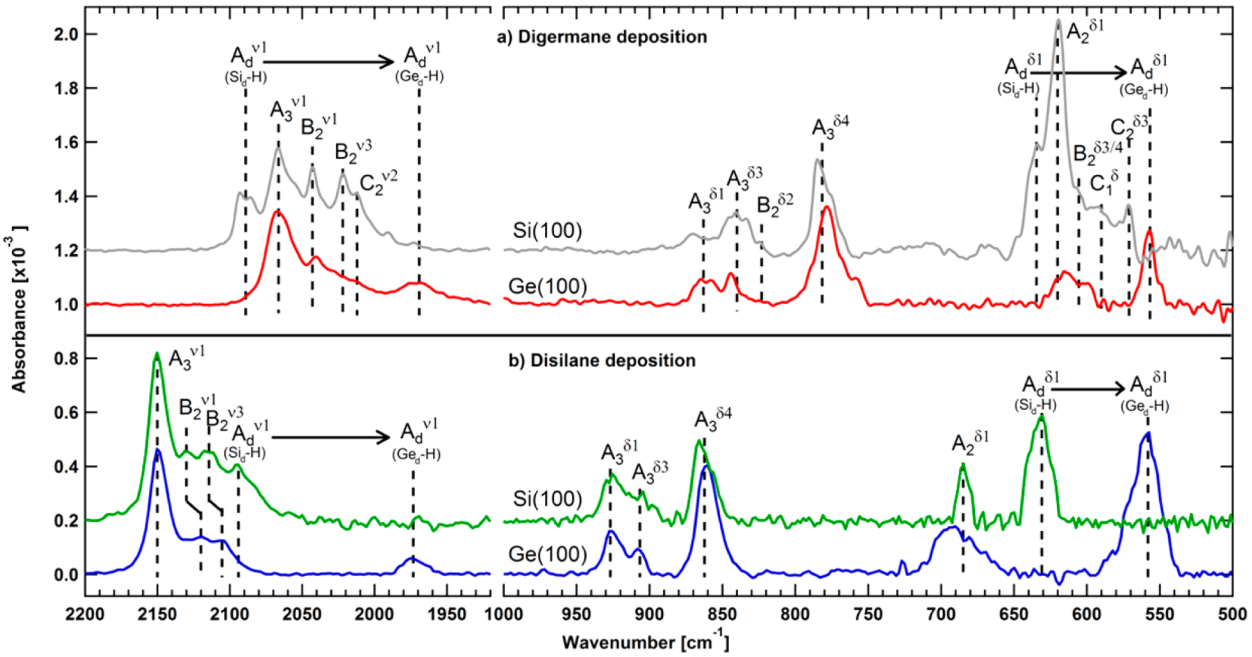

Figure 3. (a) IR adsorption spectra in absorbance of Ge_2H_6 saturated Si(100) surface (top gray curve labeled "Si(100)") and Ge(100) surface (bottom red curve labeled "Ge(100)") dosed at substrate temperature of 173 K. All of the features are identical except for the monohydrides on surface atom (Si_d or Ge_d) and the modes assigned to configuration C. (b) To aid in comparison of digermane and disilane adsorption, we reproduce the IR adsorption spectra in absorbance of Si_2H_6 saturated Si(100) surface (top green curve labeled "Si(100)") and Ge(100)surface (bottom blue curve labeled "Ge(100)") dosed at substrate temperature of 173 K[10] here. Left: vibrational stretching modes (2200−1920 cm^{-1}), right: vibrational bending modes (1000−500 cm^{-1}). All the features are identical except for the monohydride species on the surface atoms (Si_d or Ge_d).

There are, however, infrared modes near 2012, 590, and 575 cm^{-1} that appear for digermane adsorption on Si(100) and not on Ge(100) of Figure 3a). These spectral features indicate further decomposition of the digermane molecule as outlined in the Discussion section. On this basis, we assign the modes near 2012 cm^{-1} to $C_2^{\nu 2}$, 590 cm^{-1} to C_1^{δ}, and the feature near 575 cm^{-1} to $C_2^{\delta 3}$. The presence of bands corresponding to configuration C (Figure 2) upon digermane chemisorption on Si(100) and their absence when chemisorbed to Ge(100) suggest that the initial decomposition of digermane differs on these two substrates, in contrast to disilane adsorption. The initial assignment of these modes is aided by a thermal decomposition study which we show next.

2. Thermal Decomposition of ad-Germane Species. Figure 4 shows the FT-IR absorbance spectra obtained by (1) saturating a Si(100)-(2 × 1) substrate at 173 K by a saturation digermane exposure (300 L) with an effective pressure of 10^{-5} Torr at the surface, (2) annealing the substrate in vacuum from 198 to 698 K in steps of 25 K, and (3) cooling the substrate back to 173 K between each anneal step to record infrared spectra. All spectra are referenced to the clean Si(100) surface at 173 K prior to any digermane exposure. This study focuses on the spectral region above 1600 cm^{-1} because of difficulties in restoring the sample temperature exactly to 173 K (hence not able to divide out the bulk Si phonon modes at lower frequencies). Consequently, only the stretching modes in the region from 2130 to 1940 cm^{-1} are shown in Figure 4.

The initially chemisorbed Ge hydride on Si(100) species described in the previous section (dark blue curve in Figure 4) is relatively stable up to 473 K. Annealing higher than 473 K results in decomposition, leaving three absorption bands near 1990, 2060, and 2093 cm^{-1}. We have already assigned the mode near 2093 cm^{-1} to Si−H stretching vibration. The mode

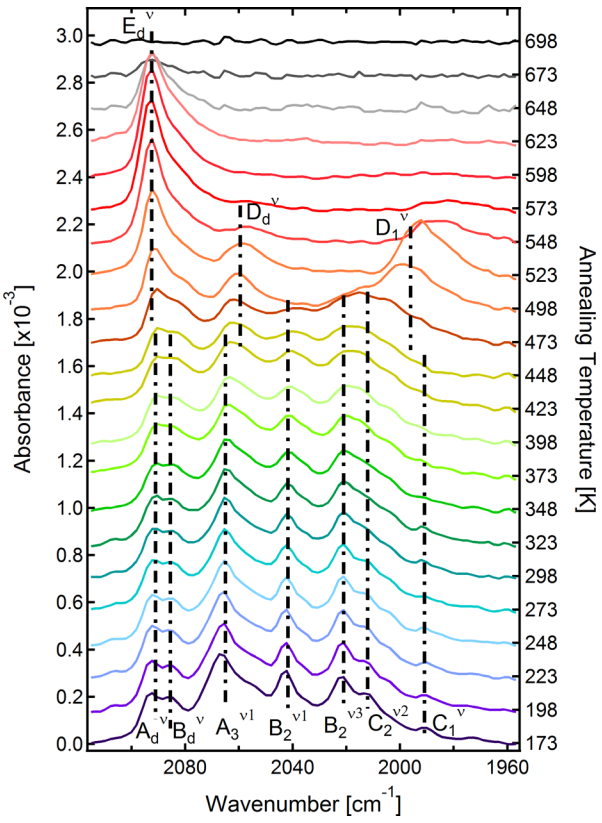

Figure 4. FT-IR spectra of digermane deposition on Si(100) at 173 K and subsequent anneals to 698 K.

near 1990 cm^{-1} is close to the Ge−H symmetric vibration mode[30] ~1995 cm^{-1} and the mode at 2062 cm^{-1} is close to a

dx.doi.org/10.1021/jp410145u | J. Phys. Chem. C 2014, 118, 482−493

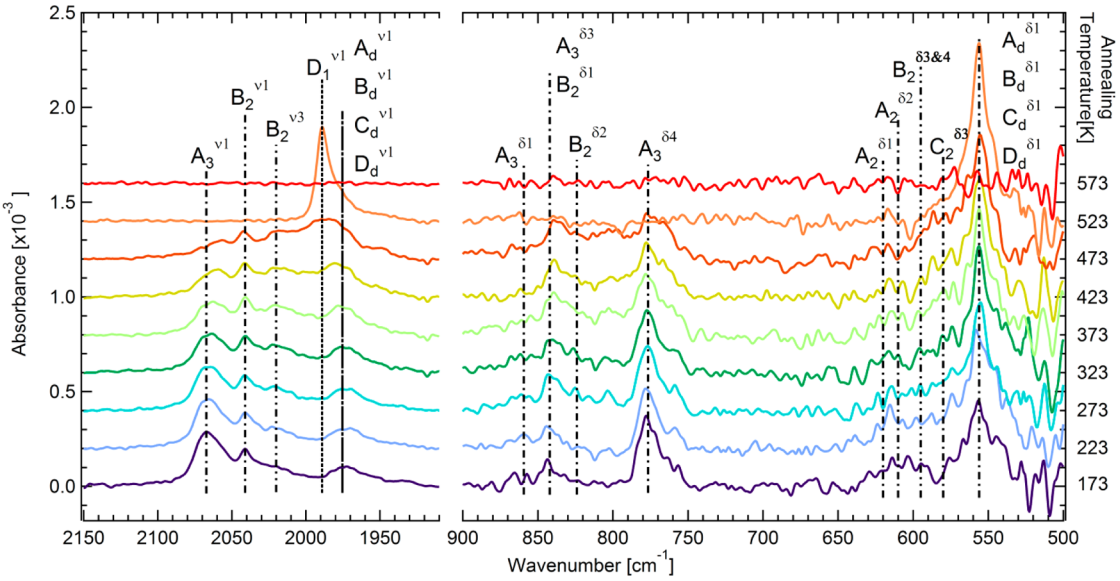

Figure 5. FT-IR spectra of digermane deposition on Ge(100) at 173 K and subsequent anneals to 573 K. For brevity, only every other anneal step is shown.

step-edge Si−H stretching mode near 2060 cm^{-1} detected previously for disilane adsorption[10] (see Figure 3a). Therefore, we assign the 1992 and 2060 cm^{-1} modes to Ge−H and step-edge Si−H stretching modes, respectively.

As the substrate temperature increases above 473 K, both the Ge−H mode near 1990 cm^{-1} and the step-edge Si−H mode near 2060 cm^{-1} increase in intensity with every annealing step until a maximum is reached at 523 K. Annealing higher than 523 K weakens these modes until their complete disappearance at 598 K. The Si−H mode near 2093 cm^{-1}, however, is present throughout the decomposition process. This mode remains stable up to 473 K, above which it intensifies slightly (see 523 K). Contrary to the behavior of the Ge−H and step-edge Si−H modes, the Si−H band near 2093 cm^{-1} intensifies while the other modes weaken upon annealing above 523 K. At 598 K, the Si−H peak near 2093 cm^{-1} reaches its maximum; it weakens upon annealing at higher temperatures and disappears at 698 K. It appears as if annealing the substrate higher than 523 K results in the migration of hydrogen from the step edge Si and Ge sites to terrace Si (Si−H mode near 2093 cm^{-1}).

The low wavenumber region could be investigated on Ge substrates because of the lower frequency phonon bands in Ge. For these experiments, a Ge(100) surface was exposed to digermane and annealed as before: (1) saturating Ge(100)-(2 × 1) substrate at 173 K with digermane using an effective pressure of 10^{-5} Torr at the surface, (2) annealing the substrate in vacuum from 198 to 573 K in steps of 25 K, and (3) cooling the substrate to 198 K between each anneal step to record infrared spectra. Note that, by selecting 198 K instead of 173 K, the temperature could be recovered more quickly, thus minimizing contamination and enhancing temperature stability during measurements without affecting the results. Since the bulk Ge phonon modes do not interfere with the bending modes of Ge−H as they do for Si, the bending region (900 to 500 cm^{-1}) can be well studied as well as the stretching region (2150 to 1910 cm^{-1}). Figure 5 shows the FT-IR absorbance spectra of these annealing cycles. All spectra are referenced to the clean Ge(100) surface at 198 K prior to digermane exposure except for the 173 K exposure that is referenced to the clean Ge(100) surface at 173 K. In keeping with our comparison of digermane exposures to that of disilane on the same substrate, we tentatively assign modes shown in Figure 5 to their disilane counterparts, postponing a more detailed discussion of these assignments to the Discussion section. The digermane modes are red-shifted about 85 cm^{-1} in the stretching region (2150 to 1910 cm^{-1}) and 70 cm^{-1} in the bending region (900 to 500 cm^{-1}) from their disilane counterparts, except of course the monohydride modes associated with hydrogen on the substrate (not associated with the initial digermane molecule any longer).

The Ge−H absorption bands associated with adsorbed digermane described in the previous section (dark blue curve in Figure 5) remain stable up to 223 K, after which the molecule gradually decomposes until only monohydrides are left on the surface at 523 K. The modes specifically associated with the Ge_2H_5 species (A_3 and A_2) gradually weaken as the annealing temperature is increased, then disappear after annealing higher than 473 K. Meanwhile, the modes associated with configuration B (Ge_2H_4) sharpen above 223 K (notably, $B_2^{\nu 3}$ near 2220 cm^{-1}). Unfortunately, except for the $B_2^{\delta 3,4}$ modes in the region of 600−580 cm^{-1}, all the modes associated with configuration B overlap with those of other configurations, complicating their assignment. At 223 K, new modes appear at 820 cm^{-1} ($C_2^{\delta 1}$) and 580 cm^{-1} ($C_2^{\delta 3}$), in addition to modes of configuration B. At 523 K, all the modes associated with the A, B, and C configurations disappear. Correspondingly, a new mode appears near 1990 cm^{-1} ($D_1^{\nu 1}$) and the peak near 560 cm^{-1} ($D_d^{\delta 1}$) reaches its highest intensity. All modes then disappear after annealing to 573 K.

3. Epitaxial Growth of Ge on Si(100) Using Digermane. In order to examine the epitaxial growth of germanium on Si(100) using digermane, a number of digermane exposures (cycles) were performed on a clean Si(100) sample followed by annealing, as described in the Experimental and Theoretical Methods section. The first and last (10th) cycles of digermane were exposed with the substrate at 173 K; all other exposures were performed with the substrate held at 373 K. The exposures performed at 173 K are used to compare the initial exposures of digermane at 173 K on Si(100) and Ge(100) surfaces. However, working at 173 K requires a

dx.doi.org/10.1021/jp410145u | J. Phys. Chem. C 2014, 118, 482−493

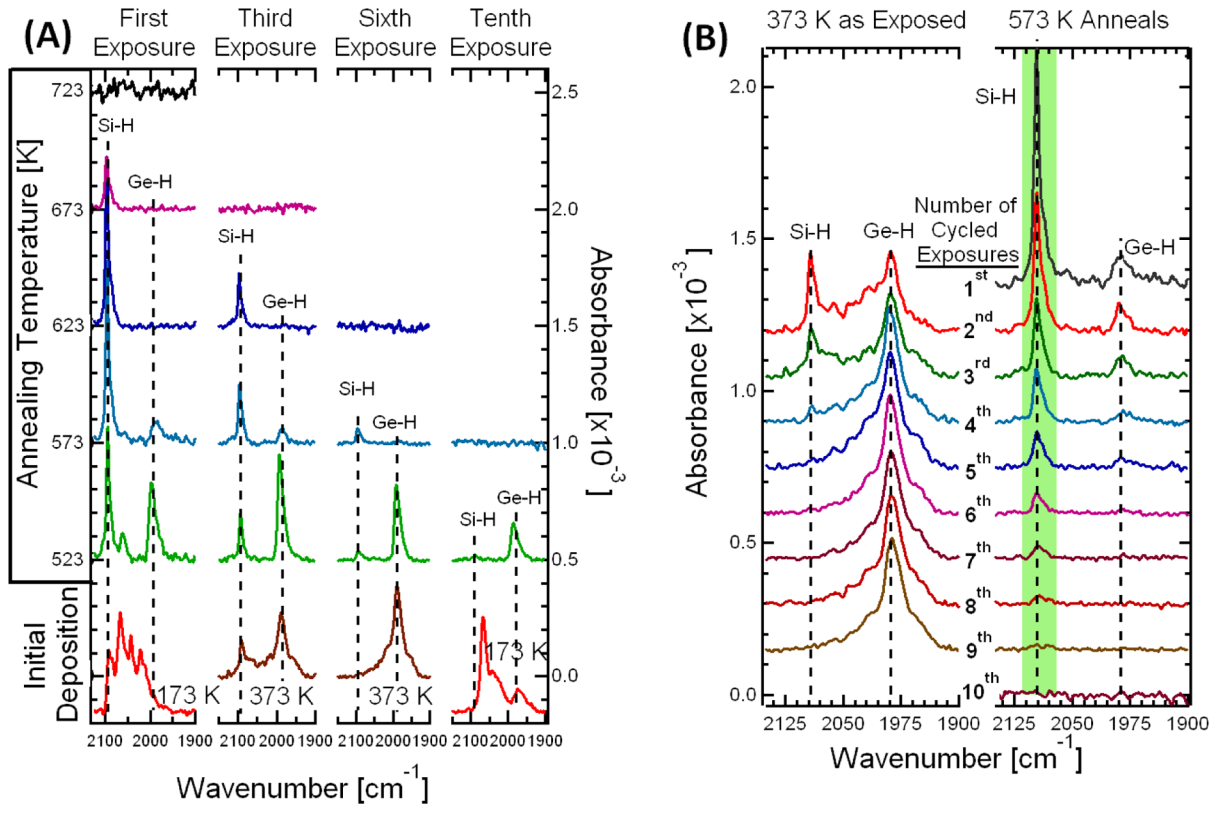

Figure 6. (A) Thermal decomposition of sequential digermane exposures. (B) The same digermane exposures as in panel A reorganized to show the differences in deposition vs 573 K anneals. The green highlighted portion corresponds to the integrated areas of the Si−H mode near 2100 cm^{-1} presented in Figure 11 and discussed in the Discussion section.

long cooling time. Therefore, to shorten the time necessary to reach the temperature for data acquisition, exposures are performed with the substrate held at 373 K (instead of 173 K) after all hydrogen has been desorbed via annealing, which minimally affects the overall amount of deposited germanium. All infrared data shown in Figures 6−8 are referenced to the fully hydrogen depassivated surface of the previous cycle at 173 K for 173 K exposures and 373 K for all others.

Figures 6a) and b) highlight the major differences of the thermal dissociation between each cycle. After each digermane/annealing cycle at or above 523 K, at most three hydride species are observed: terrace Si−H with a mode near 2093 cm^{-1} (e.g., $E_d^{\nu 1}$), step-edge Si−H with a mode near 2060 cm^{-1} (e.g., $D_d^{\nu 1}$) (in the first cycle only), and Ge−H with a mode near 1990 cm^{-1}.

Figure 6a summarizes the behavior of the Ge−H mode and the dependence of the hydrogen desorption temperature as a function of Ge coverage. The Ge−H mode is still strong at 523 K but transfers its intensity to the Si−H mode at 573 K, consistent with a migration of hydrogen from surface Ge to surface Si atoms when available (i.e., before complete Ge coverage). At high enough temperature, hydrogen desorbs from Si. For the first exposure (cycle), complete H desorption requires a 723 K anneal. This temperature steadily decreases after each new cycle, to 673 K for the third exposure, below 623 K for the sixth exposure, and 573 K for the 10th exposure. After the ninth exposure, the Si−H modes do not appear, consistent with a full Ge coverage. Therefore, the H desorption temperature corresponds to that of H on Ge(100) surfaces.

Figure 6b shows the evolution of the surface by examining the result of digermane exposures at 373 K, as a function of exposure/anneal cycles. After the second cycle, the digermane-exposed surface is characterized by two main peaks at 1990 and 2093 cm^{-1} at 373 K, assigned to the familiar Ge−H and Si−H stretching modes, respectively. As the number of cycles increases, the intensity of the Ge−H band increases slightly on the as exposed surface (at 373 K) while that of the Si−H mode decreases until it becomes undetectable by the fifth cycle. However, annealing to 573 K after each exposure results in the formation of Si−H through the ninth cycle, after which Si−H is not detectable at any annealing temperature. At that point, the surface is fully Ge covered, which can be confirmed by re-exposing digermane after the final 10th cycle of digermane at 173 K and compared to that on a clean Ge(100) surface with the same saturation dose of digermane. As shown in Figure 7, the spectra are very similar, the only difference being an enhancement in the Ge_2H_5 mode near 2067 cm^{-1}. In order to verify that the Si surface is fully covered by Ge after the ninth cycle, the substrate was titrated with atomic hydrogen at 448 K and then annealed to 573 K (Figure 8). Only Ge−H is observed until full H desorption, without formation of intermediate Si−H species.

To highlight the differences between Si and Ge and to assess the surfactant nature of the Ge overlayer, the same Ge overlayer formed by 10 digermane exposure/annealing cycles described in the prior section was exposed to disilane at 373 K and annealed to 623 K (sufficient temperature to desorb all adsorbed hydrogen). Figure 9 shows the IR absorption spectra of the initial deposition for 4 disilane/anneal cycles. After these 4 cycles, the surface was titrated with atomic hydrogen (also in Figure 9) to determine the nature of the surface atoms. The

dx.doi.org/10.1021/jp410145u | J. Phys. Chem. C 2014, 118, 482−493

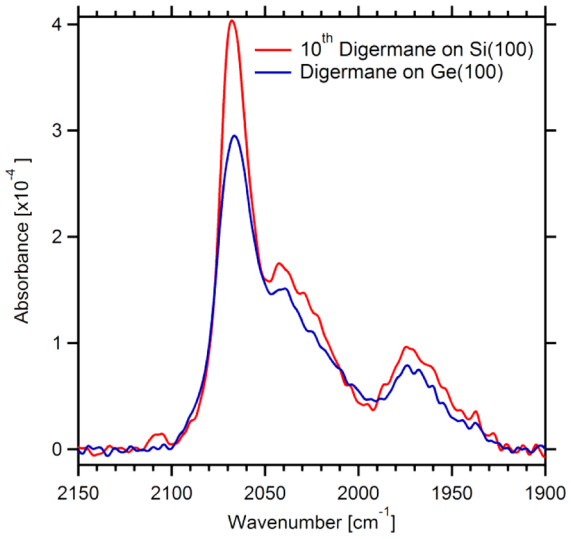

Figure 7. Saturation digermane exposure on Ge(100) at 173 K (from Figure 3a) and the last cycle of saturation digermane exposure on Si(100) at 173 K (10th).

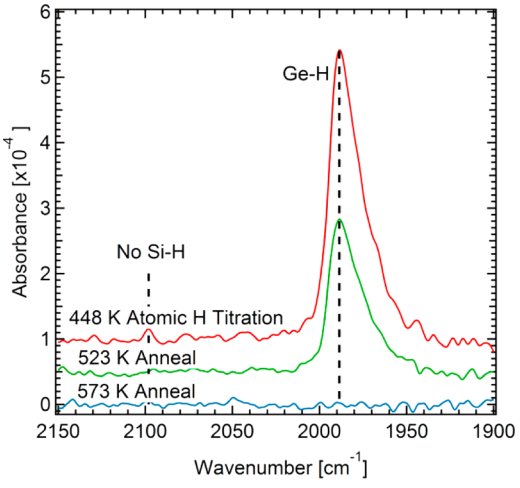

Figure 8. Titration of atomic H and thermal desorption.

atomic hydrogen titration showed only a Ge−H peak and no Si−H.

DISCUSSION

1. Initial Chemisorption of Digermane. Although Si−Si bond scission was originally proposed for disilane[20−25] adsorption on Si(100) and Ge(100) surfaces, it was recently shown that a beta-hydride elimination mechanism[10,27,28,38] is operative for disilane on both surfaces, as predicted by theoretical calculations.[17−19] The situation with digermane was less clear. Experiments had suggested that digermane adsorption involves Ge−Ge bond scission[14] while theoretical calculations[26] showed a large barrier associated with such a chemisorption pathway. Cheng et al.[26] recently showed that chemisorption of digermane on Si(100) through the β-HEP has a lower chemisorption barrier than chemisorption through Ge−Ge bond scission. The results described in the previous section help to derive an accurate picture of the adsorption process and to provide a comparison between decomposition pathways of the digermane and disilane molecules.

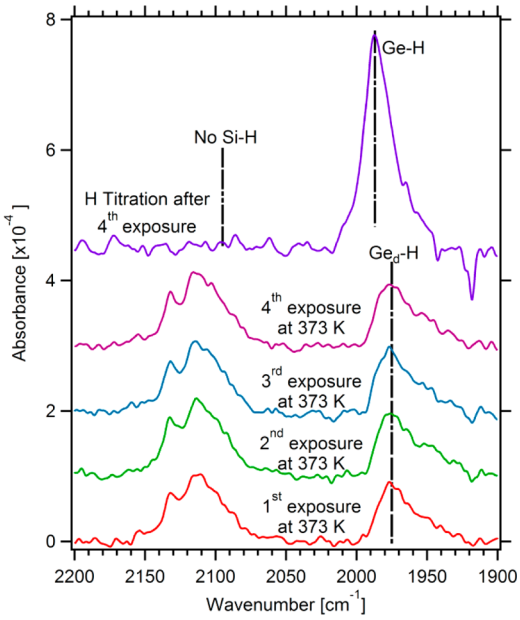

Figure 9. FT-IR spectra of cycled disilane deposition on Ge/Si(100) at 373 K. Between each deposition, the sample was annealed to 623 K to desorb all hydrogen. A final titration of atomic hydrogen was exposed to the surface at 448 K following the anneal of the last disilane exposure.

As was the case for the initial chemisorption of disilane at 173 K,[10] low temperature (173 K) deposition of digermane on Si(100) and on Ge(100) results in the appearance of dominant bands at 2090 cm^{-1} and 1975 cm^{-1}, respectively, corresponding to monohydride on the substrate atoms, Si_d-H on Si(100) and Ge_d-H on Ge(100), associated with configuration A (A_d^{ν} mode). The presence of these monohydride species at this low temperature deposition is clear evidence that the initial chemisorption is through the β-HEP mechanism ($Ge_2H_6 \rightarrow Ge_2H_5$* and −H*). If the initial chemisorption of digermane was through the Ge−Ge intra bond scission, there would be no dominant monohydride species on the surface initially, although migration of H from the precursor to the substrate could occur upon subsequent dissociation. The assignments of the monohydride species are clear from previous experiments performed on these substrates.[29,30] However, there are also more minor hydride components that tend to develop upon annealing, which require a careful assignment for a complete understanding of the mechanism.

The infrared modes of chemisorbed digermane can be assigned by a comparison with those of disilane chemisorption on the same substrates at 173 K, which are not only better known but also calculated from first principles.[10] Table 1 summarizes the measured modes of both disilane and digermane and their respective calculated values in the case of disilane. This table clearly shows that the IR modes of digermane adsorbed on Si(100) are red-shifted from their disilane counterparts in the stretching region by 85 cm^{-1} (exp) and 125 cm^{-1} (calc) and in the bending region by 70 cm^{-1} (exp) and 44 cm^{-1} (calc). Performing a correction based on these shifts and considering the vibrational band evolution resulting from subsequent decomposition (see the next section) allow for an unambiguous assignment of the modes as summarized in Table 1. There are however spectral regions with several overlapping modes. Fortunately, certain modes only appear for specific decomposition configurations. For

dx.doi.org/10.1021/jp410145u | J. Phys. Chem. C 2014, 118, 482−493

Table 1. Comparison of Calculated Disilane and Experimentally Observed Digermane Modes on a Si(100) Surface

calculated disilane IR mode[10] (cm^{-1})	configuration	observed digermane IR mode (cm^{-1})	shift (cm^{-1})
2191	$A_3^{\nu 1}$	2067	−124[a]
2177	$A_3^{\nu 2}$	2056	−121[a]
2161	$A_3^{\nu 3}$	2035	−126[a]
904	$A_3^{\delta 1}$	862	−42[b]
897	$A_3^{\delta 2}$	857	−40[b]
884	$A_3^{\delta 3}$	840	−44[b]
826	$A_3^{\delta 4}$	782	−44[b]
2169	$B_2^{\nu 1}$	2043	−126[a]
2160	$B_2^{\nu 2}$	2035	−125[a]
2153	$B_2^{\nu 3}$		
2145	$B_2^{\nu 4}$	2022	−123[a]
882	$B_2^{\delta 1}$	840	−42[b]
867	$B_2^{\delta 2}$	823	−44[b]
656	$B_2^{\delta 3}$	613	−43[b]
653	$B_2^{\delta 4}$		
2168	$C_2^{\nu 1}$	2043	−125[a]
2140	$C_2^{\nu 2}$	2012	−128[a]
889	$C_2^{\delta 1}$	847	−42[b]
664	$C_2^{\delta 2}$	620	−44[b]
619	$C_2^{\delta 3}$	572	−47[b]

[a]Shifts in the stretching region have an average of −125 cm^{-1}. [b]Shifts in the bending region have an average of −44 cm^{-1}.

example, the mode at 2067 cm^{-1} ($A_3^{\nu 1}$) is present in only configuration A, the mode at 823 cm^{-1} ($B_2^{\delta 2}$) is only present in configuration B, and the modes at 2012 cm^{-1} ($C_2^{\nu 2}$) and 575 cm^{-1} ($C_2^{\delta 3}$) are only present in configuration C. The presence of such modes is important for confirmation of the respective decomposition step on the substrate. Refinements of these mode assignments are discussed after the digermane molecule is thermally decomposed on the surface (next section).

As shown in Figure 3a, the initial deposition of digermane at 173 K differs markedly when adsorbed on Si(100) and Ge(100). From the mode assignments in Table 1, it is clear that adsorption on the Si(100) substrate results in a strong band at 2067 cm^{-1} ($A_3^{\nu 1}$) as well as features at 823 cm^{-1} ($B_2^{\delta 2}$), 2012 cm^{-1} ($C_2^{\nu 2}$), and 575 cm^{-1} ($C_2^{\delta 3}$) indicating that the initial chemisorption at 173 K involves some decomposition from the initial configuration A into configurations B and C. In contrast, adsorption on Ge(100) substrates does not produce any modes associated with configuration C at 2012 cm^{-1} ($C_2^{\nu 2}$) and 575 cm^{-1} ($C_2^{\delta 3}$), indicating that only configurations A and B are generated. The faster decomposition of digermane on Si(100) than on Ge(100) is surprising since the disilane adsorption on these same surfaces with the same flux and substrate temperatures resulted in the same level of decomposition regardless of substrate (Si(100) and Ge(100)).[10] To understand this result, a closer examination of the similarities and differences of disilane and digermane is in order.

The Si−Si bond length (2.33 Å)[39] in a disilane molecule is near that of the dimer bond length (2.25 Å)[40] on a Si(100) surface. The same is true for the Ge−Ge bond length (2.40 Å)[41] in a digermane molecule and the dimer bond length (2.44 Å)[39] on a Ge(100) surface. For this reason, the decomposition barrier of digermane on Ge(100) is expected to be low, as was found for the adsorption of disilane on Si(100).[10] Furthermore, assuming that the mismatch between the Ge−Ge and Si−Si bond lengths drive subsequent reactions (see Table 2), we expect that adsorbing digermane on Si(100) will have similar decomposition barriers to that of disilane on Ge(100). However, the nudged elastic band (NEB) calculations we performed on this system (Figure 10) indicate that digermane adsorption on Si(100) is characterized by a larger barrier (0.69 eV) from the physisorption state to configuration A than there was for disilane on Ge(100) (0.53 eV)[10] and by a lower barrier to go from configuration A to B (0.35 eV) than for disilane on Ge(100) (0.80 eV).[10] Under the same flux conditions, a higher chemisorption barrier allows for a longer amount of time for the molecule to decompose before another molecule can adsorb and interfere with the decomposition of the previously adsorbed molecule. Similarly, a lower barrier between A and B fosters the decomposition of the molecule. By analogy, digermane is expected to decompose faster on Si(100) than disilane would on Ge(100).

Table 2. Comparison of Calculated Transition Barriers for Digermane on Si(100) and for Disilane on Si(100) and Ge(100).[10]

transition configurations[a]	disilane on Si(100) (eV)[10]	disilane on Ge(100) (eV)[10]	digermane on Si(100) (eV)
Ge_2H_6 (gas) → Ge_2H_5* + H* (A)	0.14	0.53	0.69
Ge_2H_5* + H* (A) → Ge_2H_4* + 2H* (B)	0.47	0.80	0.35
Ge_2H_4* + 2H*(B) → Ge_2H_3* + 3H*(C)	2.98	2.21	2.67
Ge_2H_3* + 3H*(C) → Ge_2H_2* + 4H*(D)	2.29	1.65	2.48

[a]See Figure 10 for an illustration of the configurations.

2. Subsequent Thermal Decomposition of Ad-Germane Species. The assignments of the infrared modes of digermane in Figure 3a) are further elucidated by monitoring the thermal decomposition of the 173 K deposition. For adsorption on Si(100), the digermane species remains surprisingly stable to thermal decomposition up to a 473 K anneal (Figure 4). Above 473 K, there is evidence for decomposition by the appearance of three hydride modes: Ge−H (~1990 cm^{-1}), step-edge Si−H (~2060 cm^{-1}), and terrace Si−H (~2093 cm^{-1}). This behavior closely mimics that of the thermal decomposition of disilane on Ge(100),[10] except for the formation of configurations B and C above 323 K. While the thermal decomposition of digermane on Si(100) may be expected to be similar to disilane on Ge(100) due to similarity between Si and Ge, an NEB calculation of digermane decomposition on Si(100) (Figure 10) shows that the reaction barriers from configurations B to C and from C to D are larger than the same decomposition steps of disilane on Ge(100) (see Table 2). Above 473 K, the adsorbed digermane decomposes into configurations D and E (Figure 4). Further decomposition results in a complete removal of all Ge−H species (configuration D) and an increase in terrace Si−H (configuration E). This shows that, contrary to disilane decomposition on Ge(100),[10] hydrogen migrates away from the adsorbed Ge before desorbing from the substrate, consistent with previous work.[42−44]

The migration of hydrogen from Ge to Si makes it possible to estimate the amount of Si remaining at the surface by

dx.doi.org/10.1021/jp410145u | J. Phys. Chem. C 2014, 118, 482−493

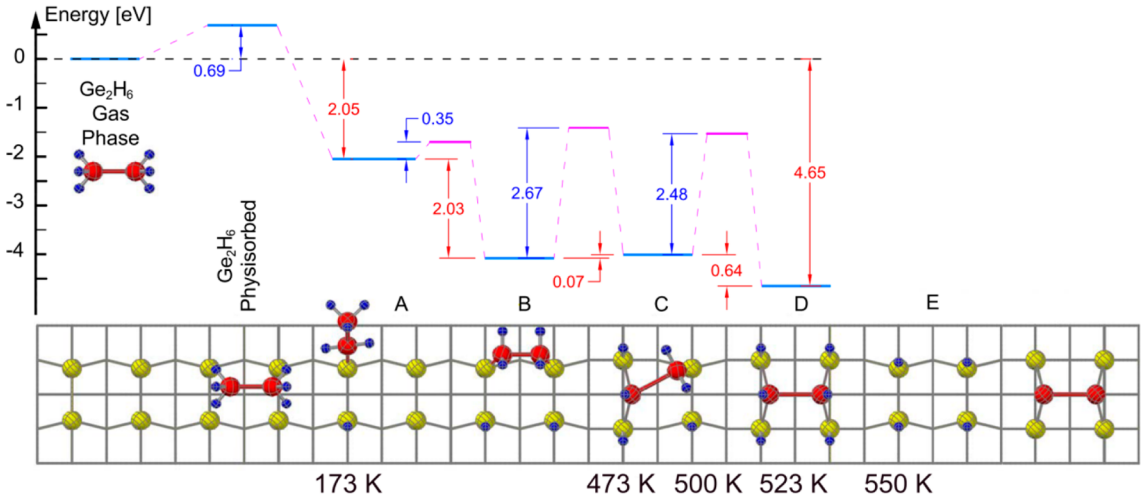

Figure 10. Proposed Thermal decomposition pathway of Ge_2H_6 on Si(100).

comparing the intensity of the Si−H band (after a 573 K anneal) to that of a fully hydrogen-passivated Si(100) surface. Such a procedure can only give a lower limit because not all surface Si atoms may be covered by hydrogen after 573 K anneal. Furthermore, we only integrate the terrace Si−H mode since the stepped edge modes are bonded to Ge adatoms (see configuration D of figure 10). Consequently, we estimate that this procedure counts only 75% ± 5% of the Si surface remaining after this initial digermane exposure (see the Supporting Information for further explanation of this calculation). Hence, we estimate that 25% of a Ge monolayer is deposited after the initial saturation digermane exposure at 173 K on Si(100).

The decomposition of digermane on Ge(100) (see Figure 5) is markedly different than on Si(100). Digermane readily decomposes with annealing as outlined in the Results section, which facilitates the assignment of the vibrational bands. The intensities of the modes at 2067 and 620 cm^{-1} decrease simultaneously with increasing temperature from 173 to 473 K while other modes stay the same or increase. These two modes can therefore be assigned to $A_3^{\nu 1}$ and $A_2^{\delta 1}$. As was pointed out in the preceding section, the frequencies of many modes of configurations expected during digermane decomposition overlap. Hence, throughout the decomposition process, the intensities of some infrared modes remain the same while those of others change gradually. We can, however track the changes in decomposition by monitoring the few modes that do not overlap. For instance, the mode at 2067 cm^{-1} is uniquely assigned to $A_3^{\nu 1}$, making it possible to quantify the evolution of that configuration (A) as the substrate is annealed from 173 to 473 K. The gradual increase (from 173 K) and rapid decline (above 473 K) of the $B_2^{\delta 2}$ mode intensity near 823 cm^{-1} point to the decomposition of configuration A into configuration B. The appearance of the mode near 580 cm^{-1} ($C_2^{\delta 3}$) at 223 K along with its gradual intensity increase up to 473 K and disappearance at 523 K indicate that configuration B starts decomposing into C at 223 K and completes the process at 473 K. The rapid disappearance of all modes except the Ge−H modes near 1990 and 560 cm^{-1} indicates that the final decomposition step before hydrogen desorption has been reached at 523 K (configuration D). At 573 K, all hydride modes disappear consistent with full hydrogen desorption observed in thermally programmed desorption (TPD) studies on Ge(100).[45]

3. Epitaxial Growth. The migration of hydrogen from Ge to Si surface atoms below the hydrogen-desorption temperature opens the door to epitaxial growth of Ge on itself. In fact, epitaxial growth of Ge on Si(100) has previously been studied under several different conditions: (1) with MBE,[46] (2) by continuous exposure of digermane with substrate temperature >450 C (above hydrogen desorption temperature),[47] and (3) repeated digermane exposures as performed here.[16] TPD experiments have shown that the hydrogen desorption temperature is lowered upon digermane exposure of Si(100) with increasing Ge coverage.[48−50] However, there have been no studies that thoroughly investigate the dependence of surface hydrogen kinetics on substrate temperature and Ge coverage, e.g., the dependence on the number of digermane exposures as reported in Figure 6a.

Consistent with prior TPD studies,[48−50] Figure 6a shows that the temperature required to desorb all hydrogen decreases with the number of digermane exposures. Additionally, above 523 K, the intensity of the Si−H band increases while that of the Ge−H band decreases. Since there is no other source of hydrogen, these data indicates that hydrogen migrates from Ge to Si surface sites or that subsurface Si swaps places with surface Ge atoms due to the presence of hydrogen.[51,52] However, the complete coverage of the surface with Ge after the ninth exposure, as evidenced by the lack of any Si−H vibration, rules out this second interpretation. The data shown in Figure 8 verify that there is in fact a full Ge coverage after the ninth exposure, since exposure to atomic hydrogen leads to Ge−H stretch absorption with no trace of Si−H vibration above the 3% monolayer sensitivity (see the Supporting Information for an explanation of this detection limit).

The migration of hydrogen from Ge to Si is evident when the Si−H and Ge−H absorption bands are compared after each exposure for 373 and 573 K anneals (Figure 6b). Since there are no external sources of hydrogen, the increase in Si−H after annealing to 573 K must be caused by the migration of hydrogen from Ge sites to Si sites left on the surface. The increase of the Si−H band after 573 K anneals can then be used to indirectly estimate the coverage of Ge where H was initially residing. This is accomplished by measuring the area of the Si−H stretch band, using the Beer−Lambert law[53] that relates the

dx.doi.org/10.1021/jp410145u | J. Phys. Chem. C 2014, 118, 482−493

absorbance of light passing through a material to the concentration of absorbing substance. For surfaces, this law is expressed in terms of coverage and dynamic dipole moment.[54] The coverage, N_s, is the only parameter that changes, which allows us to calculate the concentration by comparing it to a known standard, such as a complete H monolayer. This calculation as well as the estimation of errors is outlined in the Supporting Information.

Since the Si−H modes are only observed for H at the surface of the substrate, a fully H-terminated Si(100) surface is used as a reference. In the event that not all surface Si atoms are terminated by H, this calculation establishes a lower limit for Si coverage (Figure 11). The intensity of the Si−H stretch mode

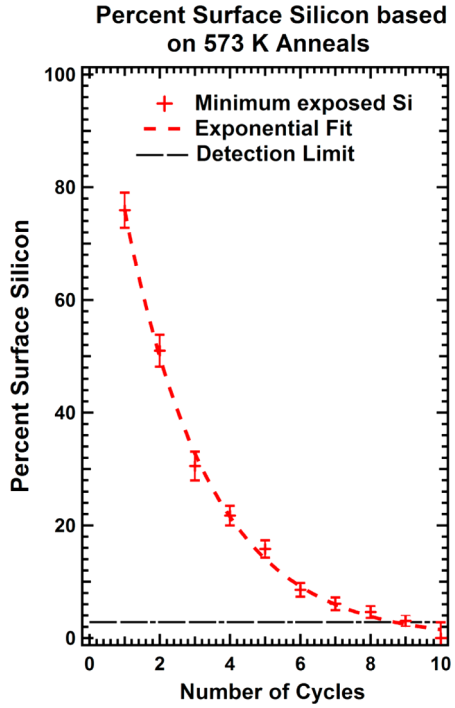

Figure 11. Percent remaining surface Si vs number of digermane cycles. Error bars represent fitting the peak areas to multiple baselines. See the Supporting Information for a description of the error bar and detection limit.

shown in Figure 11 decays exponentially with digermane exposure. Fitting these data with an exponential indicates that the amount of Si remaining on the surface decreases by ∼33% after each exposure. After the 10th cycle of exposure to digermane, the surface Si has gone below our detection limit (∼3% of a full monolayer of Si−H).

This 33% decrease of surface Si after each cycle can approximately be related the amount of Ge adsorbed if we assume that all Ge ad-atoms remain largely clustered at the surface after deposition (suggested by the functional dependence of Si−H bonds on the number of cycles) and that digermane chemisorbs on both exposed surface Ge and Si atoms. This static model of Ge ad-atoms, makes it possible to estimate that ∼33% of a monolayer of Ge is deposited per digermane cycle with the substrate held at 373 K and about 3 Ge monolayers total deposition after all 10 cycles of digermane, as detailed in the Supporting Information. This estimate of the deposition coverage per cycle was independently confirmed by RBS measurements of a sample after 15 cycles of digermane exposures on Si(100). The total surface coverage derived from these measurements was $3.0 \times 10^{15} \pm 0.1 \times 10^{15}$ Ge atoms/cm^2, consistent with 0.32 monolayers of Ge per cycle.

Figure 7 confirms that this thin Ge layer on Si(100) behaves like a bulk Ge(100) surface because the spectrum obtained upon digermane exposure at 173 K is essentially identical on both surfaces. The infrared modes for digermane deposition on the thin Ge layer are a little larger than deposition on Ge(100), but this change is well within the change in infrared intensity we have observed when adsorbing digermane on various samples of Ge(100) at 173 K.

A thin Ge layer on Si(100) has been noted to act as a surfactant to further Si deposition.[55,56] This phenomenon can be tested by examining the behavior of Si on both a thin Ge overlayer and on a bulk Ge(100) surface. As noted by Veyan et al.,[10] when disilane is deposited on bulk Ge(100), Si−H remains on the surface until all hydrogen is desorbed; after which Si diffuses into the bulk. Similarly, as we can see in Figure 9, multiple disilane exposures on this thin Ge overlayer does not result in an intensity increase of the Si−H modes upon annealing, indicating that Si diffuses below the Ge overlayer after hydrogen is desorbed from the Si. To check if there is any remaining surface Si, the annealed surface is titrated with atomic H (top of Figure 9). Only Ge−H is observed on the surface after atomic H titration, indicating that there is no surface Si, i.e., all adsorbed Si has diffused below the surface.

The temperature gap between H desorption from Ge (after a full Ge layer is formed) and complete H desorption from Si is high enough (∼150 K) that selective Ge growth can be envisioned on areas initially patterned by removal of hydrogen. Indeed, after ∼10 cycles of digermane as described above, the surface can be annealed to ∼575 K, which is much lower than the H desorption temperature for Si−H but sufficient to remove any H from the Ge overlayer, and then re-exposed at ∼400 K to digermane, thus grafting an additional ∼0.3 monolayer of Ge on that area and not on the neighboring Si surface that remains H terminated (i.e., unreactive). Further cycles of digermane exposure at ∼400 K and anneals to ∼575 K would lead to controlled Ge deposition in the patterned areas only.

This scheme is based on the knowledge (from Figure 6b) that the desorption temperature of hydrogen from Si atoms that are adjacent to Ge is higher than the desorption temperature of hydrogen on the Ge atoms themselves by at least 50 K. However, if some hydrogen could desorb in the immediate vicinity of the Ge overlayer, they would be replenished by H diffusion from the Ge atoms during the next cycle of digermane exposure and controlled annealing.

Therefore, the findings of the current study are providing a specific method for Ge ALE on nanopatterned H-terminated Si surfaces.

CONCLUSIONS AND OUTLOOK

We have shown that digermane initially chemisorbs on Si(100) and Ge(100) similarly to disilane on these same substrates, namely through a β-hydride elimination pathway decomposition mechanism with $Ge_2H_6 \rightarrow Ge_2H_5^* + H^*$. Interestingly, the initial chemisorption of digermane on Si(100) results in more subsequent decomposition at 173 K than disilane (and digermane) on Ge(100) under the same flux conditions although the initial activation barrier for digermane chemisorption on Si(100) is higher (0.69 eV) than for disilane chemisorption on Ge(100) (0.53 eV). We find that this

dx.doi.org/10.1021/jp410145u | J. Phys. Chem. C 2014, 118, 482−493

observation results from a lower calculated barrier to go from configuration A to configuration B (Ge_2H_5* + H* → *H_2Ge-GeH_2* + H* + H*, 0.25 eV) than for disilane on Ge(100) (0.80 eV), allowing for decomposition to occur even under high flux (10 langmuir/s) at low temperatures (173 K). Further thermal decomposition of digermane on Si(100) requires a substantial anneal to 473 K owing to a large decomposition barrier between configurations B and C as well as between C and D; annealing higher than 473 K results in rapid decomposition of the molecule. Thermal decomposition of digermane on Ge(100), on the other hand, occurs quite readily.

Epitaxy of Ge on Si(100) has been achieved by sequential digermane exposures and annealing cycles, and the surface hydrogen dynamics are observed as the substrate is annealed after each digermane exposure. Consistent with TPD studies,[48−50] the desorption temperature of hydrogen is lowered with increasing Ge coverage. Additionally, hydrogen is posited to migrate from adsorbed Ge to step and terrace Si atoms prior to desorption. Using hydrogen as a marker (observation of SiH modes), the amount of digermane deposited at 373 K is estimated to be 1/3 of a monolayer per cycle, as confirmed by RBS measurements. We find that 9 cycles are required to completely cover all surface Si, suggesting that Ge tend to agglomerate into islands before fully covering the Si surface.

Interestingly, this work suggests that controlled epitaxy of nanopatterned Ge structures can be achieved by controlled digermane exposure and annealing cycles, thanks to marked differences (~150 K) in hydrogen desorption temperature from Si surfaces and Ge islands as well as the hydrogen desorption temperature from Ge adlayers (573 K), which is very close to the diffusion temperature for the H on Si.[57]

■ ASSOCIATED CONTENT

Supporting Information

Explanation of errors associated with data plotted in Figure 11, the detection limit of Si−H on Si(100) using an infrared detector, and baseline corrections of infrared absorbance spectra. This material is available free of charge via the Internet at http://pubs.acs.org.

■ AUTHOR INFORMATION

Corresponding Author

*E-mail: chabal@utdallas.edu.

Notes

The authors declare no competing financial interest.

■ ACKNOWLEDGMENTS

This work has been supported by the Defense Advanced Research Project Agency (DARPA) and the Space and Naval Warfare Center, San Diego (SPAWARSYSCEN-SD) under Contract N66001-08-C-2040, and by the Texas Emerging Technology Fund of the State of Texas for the Atomically Precise Manufacturing Consortium. This work was also partially by the National Science Foundation division of Chemistry (NSF-CHE) under Grant No. 1300180. The authors acknowledge the Texas Advanced Computing Center (TACC) at The University of Texas at Austin for providing HPC resources that have contributed to the research results reported within this paper. URL: http://www.tacc.utexas.edu. The authors would also like to thank Dr. Leszek Wielunski, Rutgers University, for performing RBS measurements.

■ REFERENCES

(1) Becker, R. S.; Higashi, G. S.; Chabal, Y. J.; Becker, A. J. Atomic-Scale Conversion of Clean Si(111):H-1 × 1 to Si(111)-2 × 1 by Electron-Stimulated Desorption. *Phys. Rev. Lett.* **1990**, *65* (15), 1917−1920.

(2) Lyding, J. W.; Shen, T. C.; Hubacek, J. S.; Tucker, J. R.; Abeln, G. C. Nanoscale Patterning and Oxidation of H-Passivated Si(100)-2 × 1 Surfaces with an Ultrahigh-Vacuum Scanning Tunneling Microscope. *Appl. Phys. Lett.* **1994**, *64* (15), 2010−2012.

(3) Frank, M. M.; Chabal, Y. J.; Wilk, G. D. Nucleation and Interface Formation Mechanisms in Atomic Layer Deposition of Gate Oxides. *Appl. Phys. Lett.* **2003**, *82* (26), 4758−4760.

(4) Ho, M. T.; Wang, Y.; Brewer, R. T.; Wielunski, L. S.; Chabal, Y. J.; Moumen, N.; Boleslawski, M. In Situ Infrared Spectroscopy of Hafnium Oxide Growth on Hydrogen-Terminated Silicon Surfaces by Atomic Layer Deposition. *Appl. Phys. Lett.* **2005**, *87* (13), 133103−3.

(5) McDonnell, S. J.; Longo, R. C.; Seitz, O.; Ballard, J. B.; Mordi, G.; Dick, D. D.; Owen, J. H. G.; Randall, J. N.; Kim, J.; Chabal, Y. J.; et al. Controlling the Atomic Layer Deposition of Titanium Dioxide on Silicon: Dependence on Surface Termination. *J. Phys. Chem. C* **2013**, *117* , 20250−20259.

(6) Vinh, L. T.; Aubry-Fortuna, V.; Zheng, Y.; Bouchier, D.; Guedj, C.; Hincelin, G. UHV-CVD Heteroepitaxial Growth of $Si_{1-x}ge_x$ Alloys on Si(100) Using Silane and Germane. *Thin Solid Films* **1997**, *294* (1−2), 59−63.

(7) Gencarelli, F.; Vincent, B.; Souriau, L.; Richard, O.; Vandervorst, W.; Loo, R.; Caymax, M.; Heyns, M. Low-Temperature Ge and GeSn Chemical Vapor Deposition Using Ge_2H_6. *Thin Solid Films* **2012**, *520* (8), 3211−3215.

(8) McKay, M. R.; Shumway, J.; Drucker, J. Real-Time Coarsening Dynamics of Ge/Si(100) Nanostructures. *J. Appl. Phys.* **2006**, *99*, 9.

(9) Lin, D. S.; Wu, J. L.; Pan, S. Y.; Chiang, T. C. Atomistics of Ge Deposition on Si(100) by Atomic Layer Epitaxy. *Phys. Rev. Lett.* **2003**, *90*, 4.

(10) Veyan, J.-F.; Choi, H.; Huang, M.; Longo, R. C.; Ballard, J. B.; McDonnell, S.; Nadesalingam, M. P.; Dong, H.; Chopra, I. S.; Owen, J. H. G.; et al. Si_2H_6 Dissociative Chemisorption and Dissociation on Si(100)-(2 × 1) and Ge(100)-(2 × 1). *J. Phys. Chem. C* **2011**, *115* (50), 24534−24548.

(11) Durig, J. R.; Church, J. S. Vibrational-Spectra of Crystalline Disilane and Disilane-D6, Barrier to Internal-Rotation and Some Normal Coordinate Calculations on H3sisih3, H3sinco, and H3sincs. *J. Chem. Phys.* **1980**, *73* (10), 4784−4797.

(12) Klug, D. A.; Du, W.; Greenlief, C. M. Adsorption and Decomposition of Ge_2H_6 on Si(100). *J. Vac. Sci. Techno. A-* **1993**, *11* (4), 2067−2072.

(13) Lozano, J.; Craig, J. H., Jr; Campbell, J. H. TPD, A. HREELS, and XPS Study of Electron-Induced Deposition of Germanium on Si(100). *Appl. Surf. Sci.* **1999**, *137* (1−4), 197−203.

(14) Greenlief, C. M.; Klug, D. A.; Du, W.; Keeling, L. A., Surface Investigation of Germanium Chemical Vapor-Deposition on Silicon. In *Chemical Perspectives of Microelectronic Materials III*; Cambridge University Press: New York, 1993; Vol. *282*, pp 427−432.

(15) Lin, D. S.; Huang, K. H.; Pi, T. W.; Wu, R. T. Coverage-Dependent Thermal Reactions of Digermane on Si(100)-(2 × 1). *Phys. Rev. B* **1996**, *54* (23), 16958−16964.

(16) Huang, K. H.; Ku, T. S.; Lin, D. S. Growth Process of Ge on Si(100)-(2 × 1) in Atomic-Layer Epitaxy from Ge2h6. *Phys. Rev. B* **1997**, *56* (8), 4878−4886.

(17) Cho, H. C. Ge Deposition from Digermane on the Si(100)-(2 × 1) Surface. *Appl. Surf. Sci.* **1996**, *92*, 128−131.

(18) Lu, G.-Q. *Group IV Semiconductor Surface Chemistry: A Multiple Internal Reflection Infrared Spectroscopy Study*; University of California, San Diego: San Diego, CA, 1992.

(19) Shinohara, M.; Seyama, A.; Kimura, Y.; Niwano, M.; Saito, M. Formation and Decomposition of Si Hydrides During Adsorption of Si_2H_6 onto Si(100)(2 × 1). *Phys. Rev. B* **2002**, *65* (7), 075319.

(20) Suda, Y. Migration-Assisted Si Subatomic-Layer Epitaxy from Si_2H_6. *J. Vac. Sci. Technol. A* **1997**, *15* (5), 2463−2468.

(21) Wu, Y. M.; Baker, J.; Hamilton, P.; Nix, R. M. Mirirs Studies of the Growth of Si and Si-Ge Alloys from Molecular Precursors. *Surf. Sci.* **1993**, *295* (1−2), 133−142.
(22) Akazawa, H.; Utsumi, Y. Reaction Kinetics in Synchrotron-Radiation-Excited Si Epitaxy with Disilane. II. Photochemical-Vapor Deposition. *J. Appl. Phys.* **1995**, *78* (4), 2740−2750.
(23) Owen, J. H. G.; Miki, K.; Bowler, D. R.; Goringe, C. M.; Goldfarb, I.; Briggs, G. A. D. Gas-Source Growth of Group IV Semiconductors: I. Si(001) Nucleation Mechanisms. *Surf. Sci.* **1997**, *394* (1−3), 79−90.
(24) Wang, Y.; Bronikowski, M. J.; Hamers, R. J. An Atomically Resolved Scanning Tunneling Microscopy Study of the Thermal Decomposition of Disilane on Si(001). *Surf. Sci.* **1994**, *311* (1−2), 64−100.
(25) Bozso, F.; Avouris, P. Thermal and Electron-Beam-Induced Reaction of Disilane on Si(100)-(2 × 1). *Phys. Rev. B* **1988**, *38* (6), 3943−3947.
(26) Cheng, C.-L.; Tsai, D.-S.; Jiang, J.-C. Energetics and Rate Constants of Si_2H_6 and Ge_2H_6 Dissociative Adsorption on Dimers of SiGe(100)-2 × 1. *J. Phys. Chem. C* **2007**, *111* (36), 13466−13472.
(27) Shi, J.; Tok, E. S.; Kang, H. C. The Dissociative Adsorption of Silane and Disilane on Si(100)-(2 × 1). *J. Chem. Phys.* **2007**, *127* (16), 164713−12.
(28) Ng, R. Q.-M.; Tok, E. S.; Kang, H. C. Disilane Chemisorption on Si_XGe_{1-X}(100)-(2 × 1): Molecular Mechanisms and Implications for Film Growth Rates. *J. Chem. Phys.* **2009**, *131* (4), 044707−8.
(29) Chabal, Y. J.; Christman, S. B. Evidence of Dissociation of Water on the Si(100)2 × 1 Surface. *Phys. Rev. B* **1984**, *29* (12), 6974−6976.
(30) Chabal, Y. J. High-Resolution Infrared Spectroscopy of Adsorbates on Semiconductor Surfaces: Hydrogen on Si(100) and Ge(100). *Surf. Sci.* **1986**, *168* (1−3), 594−608.
(31) Jónsson, H.; Mills, G.; Jacobsen, K. W. Nudged Elastic Band Method for Finding Minimum Energy Paths of Transitions. In *Classical and Quantum Dynamics in Condensed Phase Simulations*, World Scientific: Singapore, 1998; pp 385−404.
(32) Kresse, G.; Hafner, J. Ab Initio Molecular Dynamics for Liquid Metals. *Phys. Rev. B* **1993**, *47* (1), 558−561.
(33) Kresse, G.; Furthmüller, J. Efficient Iterative Schemes for Ab Initio Total-Energy Calculations Using a Plane-Wave Basis Set. *Phys. Rev. B* **1996**, *54* (16), 11169−11186.
(34) Kresse, G.; Joubert, D. From Ultrasoft Pseudopotentials to the Projector Augmented-Wave Method. *Phys. Rev. B* **1999**, *59* (3), 1758−1775.
(35) Perdew, J. P.; Wang, Y. Accurate and Simple Analytic Representation of the Electron-Gas Correlation Energy. *Phys. Rev. B* **1992**, *45* (23), 13244−13249.
(36) Vanderbilt, D. Soft Self-Consistent Pseudopotentials in a Generalized Eigenvalue Formalism. *Phys. Rev. B* **1990**, *41* (11), 7892−7895.
(37) Monkhorst, H. J.; Pack, J. D. Special Points for Brillouin-Zone Integrations. *Phys. Rev. B* **1976**, *13* (12), 5188−5192.
(38) Xia, L. Q.; Jones, M. E.; Maity, N.; Engstrom, J. R. Dissociation and Pyrolysis of Si_2H_6 on Si Surfaces: The Influence of Surface Structure and Adlayer Composition. *J. Chem. Phys.* **1995**, *103* (4), 1691−1701.
(39) Rossmann, R.; Meyerheim, H. L.; Jahns, V.; Wever, J.; Moritz, W.; Wolf, D.; Dornisch, D.; Schulz, H. The Ge(001) (2 × 1) Reconstruction: Asymmetric Dimers and Multilayer Relaxation Observed by Grazing Incidence X-Ray Diffraction. *Surf. Sci.* **1992**, *279* (1−2), 199−209.
(40) Yin, M. T.; Cohen, M. L. Theoretical Determination of Surface Atomic Geometry: Si(001)-(2 × 1). *Phys. Rev. B* **1981**, *24* (4), 2303−2306.
(41) Beagley, B.; Monaghan, J. J. Electron Diffraction Study of Digermane. *Trans. Faraday Soc.* **1970**, *66* (0), 2745−2748.
(42) Hirose, F.; Sakamoto, H.; Terashi, M.; Kuge, J.; Niwano, M. Hydrogen Adsorption and Desorption on SiGe Investigated by in Situ Surface Infrared Spectroscopy. *Thin Solid Films* **1999**, *343*−*344* (0), 404−407.
(43) Tok, E. S.; Ong, S. W.; Kang, H. C. Hydrogen Desorption Kinetics from the $Si_{1-X}Ge_X$(100)-(2 × 1) Surface. *J. Chem. Phys.* **2004**, *120* (11), 5424−5431.
(44) Li, Q.; Tok, E. S.; Zhang, J.; Kang, H. C. Reassessment of the Molecular Mechanisms for H_2 Thermal Desorption Pathways from $Si_{1-X}Ge_X$(001)-(2 × 1) Surfaces. *J. Chem. Phys.* **2007**, *126* (4), 044706−15.
(45) Lewis, L. B.; Segall, J.; Janda, K. C. Recombinative Desorption of Hydrogen from the Ge(100)−(2 × 1) Surface: A Laser-Induced Desorption Study. *J. Chem. Phys.* **1995**, *102* (18), 7222−7228.
(46) Eaglesham, D. J.; Cerullo, M. Low-Temperature Growth of Ge on Si(100). *Appl. Phys. Lett.* **1991**, *58* (20), 2276−2278.
(47) Kim, H.; Taylor, N.; Bramblett, T. R.; Greene, J. E. Kinetics of $Si_{1-X}Ge_X$ (001) Growth on Si(001)2 × 1 by Gas-Source Molecular-Beam Epitaxy from Si_2H_6 and Ge_2H_6. *J. Appl. Phys.* **1998**, *84* (11), 6372−6381.
(48) Ning, B. M. H.; Crowell, J. E. Investigation on the Growth Rate Enhancement by Ge During SiGe Alloy Deposition by Chemical Vapor Deposition. *Appl. Phys. Lett.* **1992**, *60* (23), 2914−2916.
(49) Russell, N. M.; Ekerdt, J. G. Kinetics of Hydrogen Desorption from Germanium-Covered Si(100). *Surf. Sci.* **1996**, *369* (1−3), 51−68.
(50) Angot, T.; Louis, P. Hydrogen Population on Ge-Covered Si(001) Surfaces. *Phys. Rev. B* **1999**, *60* (8), 5938−5945.
(51) Rudkevich, E.; Liu, F.; Savage, D. E.; Kuech, T. F.; McCaughan, L.; Lagally, M. G. Hydrogen Induced Si Surface Segregation on Ge-Covered Si(001). *Phys. Rev. Lett.* **1998**, *81* (16), 3467−3470.
(52) Kobayashi, Y.; Sumitomo, K.; Shiraishi, K.; Urisu, T.; Ogino, T. Control of Surface Composition on Ge/Si(001) by Atomic Hydrogen Irradiation. *Surf. Sci.* **1999**, *436* (1−3), 9−14.
(53) Ingle, J. D.; Crouch, S. R., *Spectrochemical Analysis*; Prentice Hall: Saddle River, NJ, 1988; p 608.
(54) Chabal, Y. J. Surface Infrared Spectroscopy. *Surf. Sci. Rep.* **1988**, *8* (5−7), 211−357.
(55) Fukatsu, S.; Fujita, K.; Yaguchi, H.; Shiraki, Y.; Ito, R. Self-Limitation in the Surface Segregation of Ge Atoms During Si Molecular Beam Epitaxial Growth. *Appl. Phys. Lett.* **1991**, *59* (17), 2103−2105.
(56) Lam, A. M.; Zheng, Y. J.; Engstrom, J. R. Direct in Situ Characterization of Ge Surface Segregation in Strained $Si_{1-X}Ge_X$ Epitaxial Thin Films. *Appl. Phys. Lett.* **1998**, *73* (14), 2027−2029.
(57) Owen, J. H. G.; Bowler, D. R.; Goringe, C. M.; Miki, K.; Briggs, G. A. D. Hydrogen Diffusion on Si(001). *Phys. Rev. B* **1996**, *54* (19), 14153−14157.